water

MDPI

Article

Trend Analysis of Rainfall Using Gridded Data over a Region of Southern Italy

Tommaso Caloiero [1], Roberto Coscarelli [2,*] and Gaetano Pellicone [1]

[1] National Research Council—Institute for Agricultural and Forest Systems in Mediterranean (CNR-ISAFOM), 87036 Rende, Italy; tommaso.caloiero@isafom.cnr.it (T.C.); gpellicone@gmail.com (G.P.)
[2] National Research Council—Research Institute for Geo-Hydrological Protection (CNR-IRPI), 87036 Rende, Italy
* Correspondence: roberto.coscarelli@irpi.cnr.it; Tel.: +39-0984-841-417

Abstract: Climate change is affecting all regions worldwide. Globally, polar ice shields are melting and the sea is rising. Moreover, some regions are facing more common extreme weather events and rainfall, while others are experiencing more extreme heat waves and droughts, causing changes in mean renewable water supplies e.g., precipitation and runoff. In this work, in order to detect possible rainfall trends in the Calabria region (southern Italy), a gridded database has been obtained from a rainfall data set of 129 monthly series collected for the period 1951–2016. In particular, the Inverse Distance Weighed was applied to build 603 rainfall grid series with a spatial resolution of 5 km × 5 km and, for each grid point, the monthly, seasonal and annual rainfall series were analyzed with the Mann–Kendall non-parametric test and the Theil–Sen estimator. Results showed a decreasing trend for the annual and winter–autumn rainfall and an increasing trend for the summer one.

Keywords: rainfall; IDW; trend; Mann–Kendall; Calabria

Citation: Caloiero, T.; Coscarelli, R.; Pellicone, G. Trend Analysis of Rainfall Using Gridded Data over a Region of Southern Italy. *Water* **2021**, *13*, 2271. https://doi.org/10.3390/w13162271

Academic Editors: Vasilis Kanakoudis and Stavroula Tsitsifli

Received: 6 August 2021
Accepted: 17 August 2021
Published: 19 August 2021

1. Introduction

Climate in the Mediterranean is influenced by the arid North African currents and by Central Europe's temperate, humid ones. As a result, the Mediterranean basin emerges as one of the most affected areas by climate change, with rising temperatures and decreasing rainfall significantly altering rainfall distribution across time and space [1]. Therefore, several analyses on the precipitation distribution in the Mediterranean basin have been performed both at large [2,3] and regional scale [4–6]. Generally, a large number of studies revealed a negative trend of yearly total and average precipitation in the Mediterranean basin and consequently an increase in drought events, especially since the second half of the past century [7]. Several authors [8,9] have shown different trends among the four seasons: negative tendencies in autumn and winter, positive ones in summer. Peña-Angulo et al. [10], in a study on long-term precipitation trend in Southwestern Europe for the period 1850–2018, found significant trends only for short periods, evidencing strong interannual and decadal variability at the annual and seasonal scales. Various studies carried out on both regional and local scales [11,12] have shown an increase in the frequency of extreme rainfall and temperature events such as heat waves, floods, droughts. An increase in dry days, associated with a positive trend in rainfall intensity, has been evidenced in areas characterized by Mediterranean climate by Polade et al. [13]: this means that where dry periods are longer, extreme rainfall events could be more frequent.

The analysis of rainfall trends in mountainous areas are very interesting for the high variability characterizing these zones and useful for several reasons, such as the generation of runoff and eroded materials, mainly after very intense rainfall events. Stefanidis and Stathis [14] analyzed the rainfall trends in the Mountainous Central Pindus of Greece detecting decreasing tendencies on the annual scale and in Winter and Spring, and positive trends in Autumn and Summer, reaching to an average magnitude of +2.4%.

In order to accurately describe the spatial tendencies of climate variables, it is necessary to have a network of properly distributed stations. Even though the World Meteorological Organization provided useful guidelines for building such networks, they often lack in the distribution of stations due to various factors (orography, costs, constant powering and connection to internet, security, etc.). To overcome these problems, it is necessary to build a grid series, which are increasingly being used as inputs for trend detection, modelling, statistical analysis, etc. [15]. Various studies on gridded database have been developed worldwide analyzing the sets comparatively and in accordance with the correlation value between estimated and observation data [16–18]. Darand and Khandu [19] estimated the accuracy of 23 globally and regionally gridded products of rainfall for Iran, classifying them into five categories based on the sources of data: gauge-only, gauge-satellite, gauge-reanalysis, reanalysis-only, and gauge-satellite-reanalysis. Yao et al. [20] in a study referred to northwestern China have shown that all the gridded precipitation datasets, used in their analysis, well reproduce the climatology, the variability and the spatiotemporal patterns of rainfall, but conversely evidenced discrepancies in the long-term trend detection. Abdourahamane [21] analyzed the reliability of gridded rainfall products of an observation network in Niger considering four gridded datasets. In the mountainous Joumine catchment (northern Tunisia) Aouissi et al. [22] analyzed the influence of both rainfall variability and catchment subdivision on streamflow by means of an option set of rain gauges (SWAT model) with the aim to investigate the balance among hydrometeorological variability, data scarcity and flexibility.

In this study, in order to detect possible changes in rainfall data in a region of southern Italy (Calabria), for the high spatial density of the station network, a monthly gridded database with a resolution 5 km × 5 km has been built overcoming some problems that affect the more diffuse global gridded datasets. In this way, a better spatial analysis of the trends has been carried out by using two non-parametric tests.

2. Study Area and Data

Due to its position, in the center of the Mediterranean basin, and to its climatic characteristics, Calabria is considered a highly susceptible area to climate change, where even a small temperature increase could lead to various environmental problems. The Calabria region is located between 37°54′ and 40°09′ N and between 15°37′ and 17°13′ E, with an area of 15,080 km^2 [23]. The region presents a north–south oriented long shape and, although it does not have many high peaks, it is one of the most mountainous Italian regions, with mountains occupying 42% of the region and hills covering 49% of the territory (Figure 1). The Köppen–Geiger classification [24] identifies the climate of the region as a hot-summer Mediterranean climate, therefore with relatively mild winters (with rain) and very hot summers (often very dry). With this climate, the coldest month generally has average temperature above 0 °C, at least 1 month's average temperature reaches values higher than 22 °C, and at least 4 months present average temperature above 10 °C. Moreover, due to its orography, the region presents sharp contrasts, with the warm air currents coming from Africa affecting the Ionian side with short and heavy precipitations, and the western air currents affecting the Tyrrhenian side with high precipitation amounts [25].

In this study, a database of 603 monthly rainfall gridded series, with a spatial resolution of 5 km × 5 km, was obtained from the original rainfall database managed by the Multi-Risk Functional Centre of the Regional Agency for Environment Protection of the Calabria region. These series have been checked to detect and correct inhomogeneities and to fill in missing data only for the period 1923–2006 by Brunetti et al. [8]. In this study, only 129 homogenous and filled datasets have been updated to 2016 after a posteriori check to verify if the time series are statistically homogeneous also in the period 2007–2016. Indeed, no new inhomogeneities have been detected and thus in this study the 129 monthly rainfall series (about one station per 117 km^2) for the period 1951–2016 have been analyzed and spatially distributed to build 603 monthly rainfall grid series (Figure 1). As a result, the study period is different from the one proposed in Brunetti et al. [8] because it starts and

ends in years different from the previous study. In fact, in order to perform a reliable spatial analysis, the same number of stations must be considered for each year, and thus, in this paper, 1951 has been chosen as first year. In fact, before 1951, the number of stations considered in Brunetti et al. [8] significantly differ from one year to another.

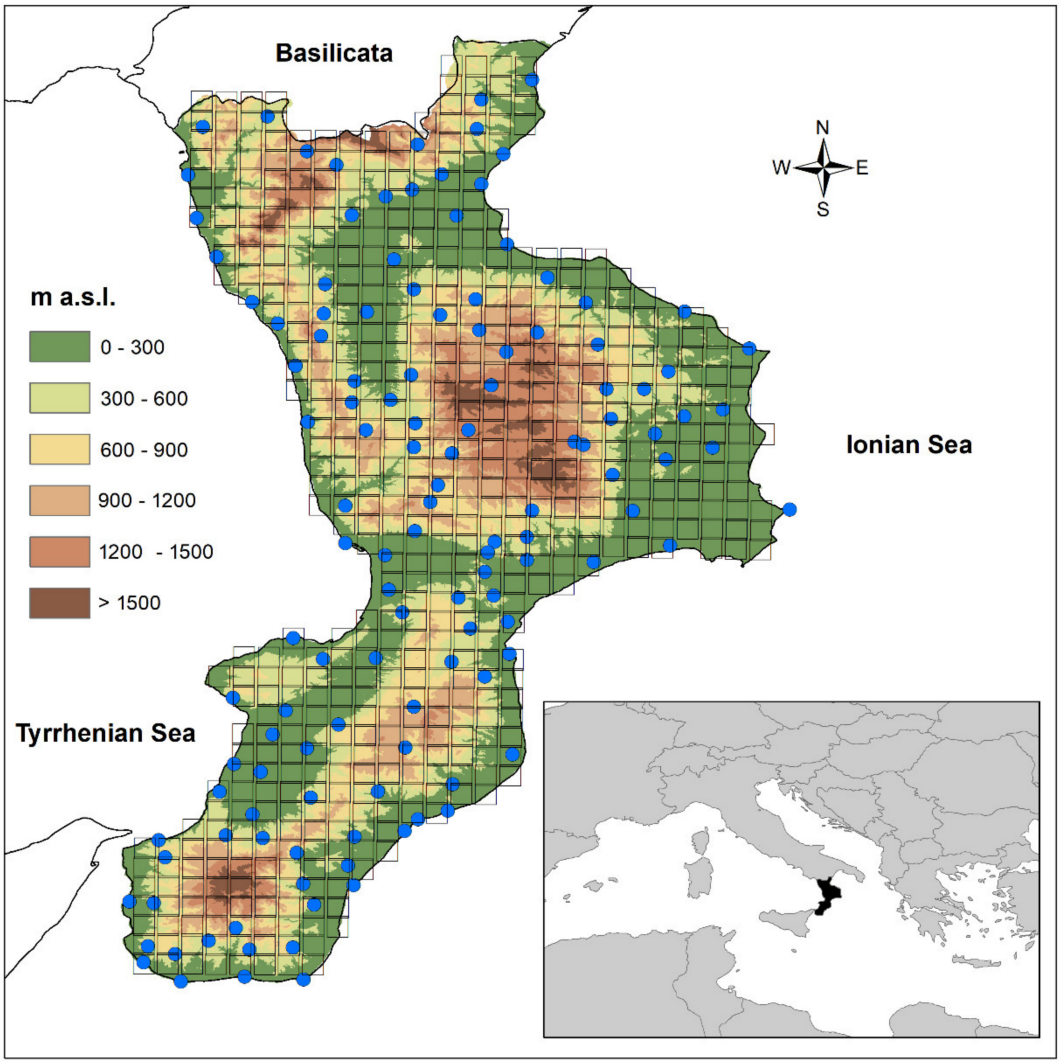

Figure 1. Localization of the rain gauges on a Digital Elevation Model of the Calabria region and visualization of the grid with a spatial resolution of 5 km × 5 km.

3. Methods

3.1. Inverse Distance Weighed

The database of 603 monthly rainfall grid series with a spatial resolution of 5 km × 5 km has been obtained by means of the Inverse Distance Weighed (IDW) that is based on the algorithm of [26,27]. Even though IDW is a fairly easy deterministic interpolation technique, it has been used in numerous studies. For example, Dirks et al. [28] compared the performance of IDW and kriging in interpolating rainfall data, recommending IDW for spatially dense networks of rain gauges. In fact, although geostatistical interpolators outperform the IDW, the rainfall spatial distribution for spatially dense networks of rain gauges gave fairly satisfactory results [29].

The IDW relates the unknown value of a certain variable in a defined point to the values of the same variable measured in other locations, based on the distance between the

locations. The closer an observation is to the point of estimate, the higher its influence that is expressed through a weight (w), given by:

$$w_i(x) = \frac{1}{d(x, x_i)^p} \tag{1}$$

where x is the point in which rainfall is unknown, x_i is one of the points in which rainfall is available, d is the distance between the two points, and p is an exponent that allows to give different forms to the weighting function. The higher p is, the less importance is given to more remote observations. In this study, with the aim to not penalize too much the contribution to the estimate of distant points, p was set equal to 2. Moreover, the number of observations used for each estimation was set to 12.

3.2. Theil–Sen Estimator

The Theil–Sen estimator (TSE) is generally considered more powerful than linear regression methods in trend magnitude evaluation, because it is not subject to the influence of extreme values [30]. Given $x_1, x_2, \ldots, x_n$ rainfall observations at times $t_1, t_2, \ldots, t_n$ (with $t_1 < t_2 < \ldots < t_n$), for each N pairs of observations x_j and x_i taken at times t_j and t_i, the gradient Q_k can be calculated as:

$$Q_k = \frac{x_j - x_i}{t_j - t_i} \quad for \quad k = 1, \ldots, N \tag{2}$$

with $1 < i < j < n$ and $t_j > t_i$.

The estimate of trend in the data series $x_1, x_2, \ldots, x_n$ can then be calculated as the median Q_{med} of the N values of Q_k, ranked from the smallest to the largest:

$$Q_{med} = \begin{cases} Q_{[(N+1)/2]} & if\ N\ is\ odd \\ \frac{Q_{[N/2]} + Q_{[(N+2)/2]}}{2} & if\ N\ is\ even \end{cases} \tag{3}$$

The Q_{med} sign reveals the trend behavior, while its value indicates the magnitude of the trend.

3.3. Mann-Kendall Test

As regards the MK test [31,32], in order to evaluate the trend significance, the statistic S based on rank sums is calculated as:

$$S = \sum_{i=1}^{n-1} \sum_{j=i+1}^{n} sgn(x_j - x_i) \ \ where \ \ sgn(x_j - x_i) = \begin{cases} 1 & if \quad (x_j - x_i) > 0 \\ 0 & if \quad (x_j - x_i) = 0 \\ -1 & if \quad (x_j - x_i) < 0 \end{cases} \tag{4}$$

In which x_j and x_i are the observations taken at times j and i (with $j > i$), respectively, and n is the dimension of the series.

Under the null hypothesis H_0, the distribution of S is symmetrical and is normal in the limit as n becomes large, with zero mean and variance:

$$Var(S) = \left[n\,(n-1)\,(2\,n+5) - \sum_{i=1}^{m} t_i\,(t_i - 1)\,(2\,t_i + 5) \right] / 18 \tag{5}$$

in which t_i indicates the number of ties with extend i.

Given the variance of S, it is possible to evaluate the standardized statistic Z_{MK} as:

$$Z_{MK} = \begin{cases} \frac{S-1}{\sqrt{Var(S)}} & for\ S > 0 \\ 0 & for\ S = 0 \\ \frac{S+1}{\sqrt{Var(S)}} & for\ S < 0 \end{cases} \tag{6}$$

By applying a two-tailed test, for a specified significance level α, the significance of the trend can be evaluated. In particular, in this work, the rainfall series have been examined for a significance level (SL) equal to 95%.

4. Results

Figure 2a shows a synthesis of the results of the trend analysis applied to the annual, seasonal and monthly rainfall as percentages of grid points presenting a positive or a negative trend. Results showed a clear annual negative trend. In fact, more than 54%, and only 1%, of the grid points evidenced decreasing and increasing tendencies, respectively. Spatially, the negative trend has been detected throughout the entire region but, particularly, in the northwestern side, where magnitudes lower than −50 mm/10 years have been evaluated in several grid points (Figure 2b). Moreover, important negative trends values have been also identified in the central and in the southwestern side of the region, with magnitudes always lower than −50 mm/10 years. Conversely, the Ionian side of the region is characterized by a positive trend of the annual rainfall even though with increasing values between 40 and 50 mm/10 years (Figure 2b).

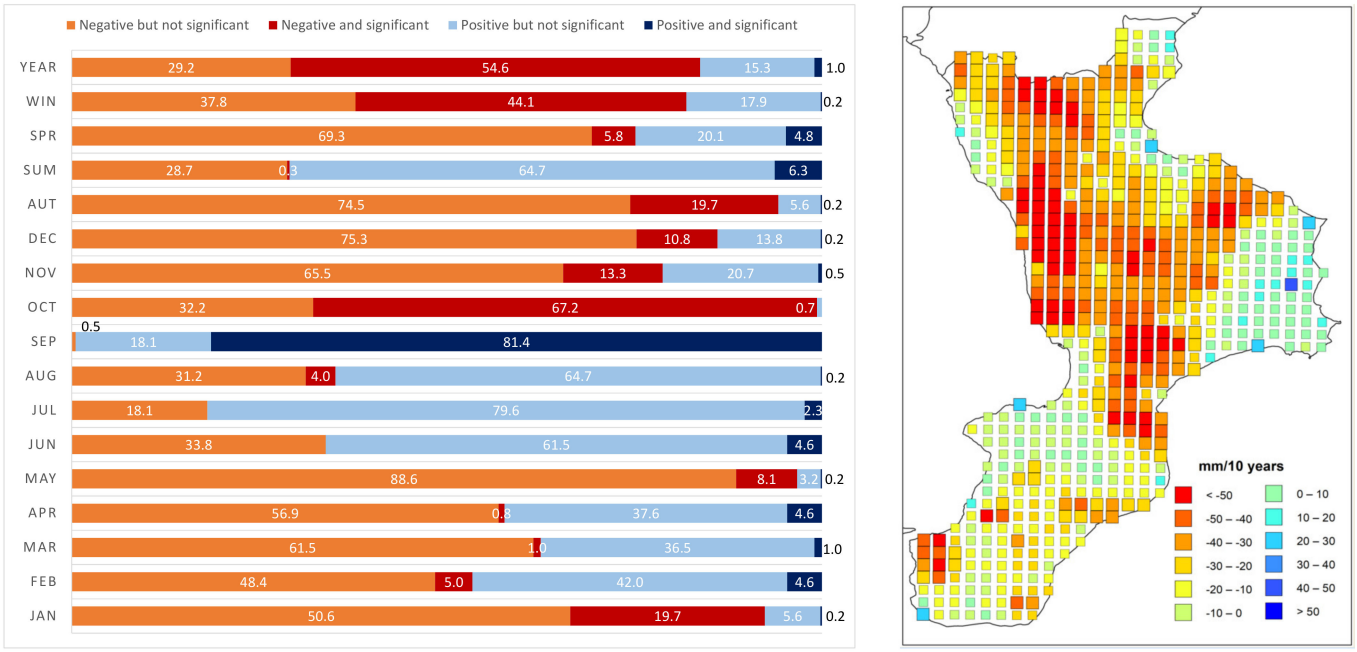

(**a**) (**b**)

Figure 2. (**a**) Percentages of grid points presenting positive or negative trend; (**b**) Annual trend map. Squares dimension indicates the significance level of the trend: large squares $p < 0.05$, small squares otherwise.

The analysis of the seasonal tendencies showed that the negative trend of the annual rainfall is mainly due to the negative rainfall reduction detected in winter, with about 44% of the grid points showing significant negative values and only 0.2% presenting an opposite behavior (Figure 2a).

The negative trend behavior detected at seasonal scale has been confirmed in the winter months separately (i.e., December, January and February), in particular in December and January, with 10.8% and 19.7% of the grid points showing negative tendencies, respectively, and only 0.2% of the grid points presenting a positive trend (Figure 2a). In February, the number of grid points presenting positive (4.6% of the grid points) or negative (5.0%) trends are quite similar. Spatially, results of the trend analysis applied to the winter rainfall (Figure 3) evidenced a similar distribution of the corresponding distribution of the annual scale (Figure 2b) for the negative values. In fact, in winter, rainfall decreases, reaching

values lower than −20 mm/10 years, have been detected in the northwestern, central and in the southwestern side of the region (Figure 3).

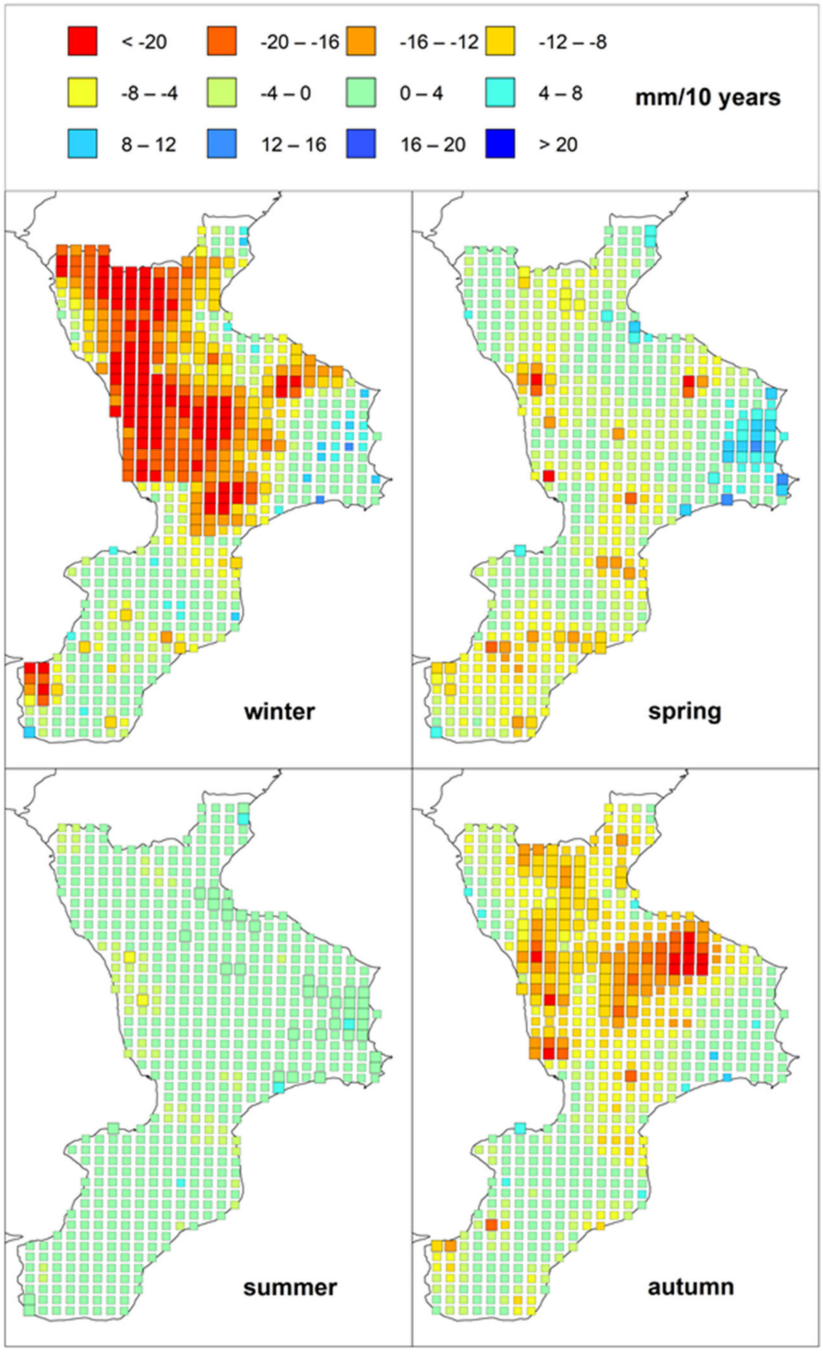

Figure 3. Seasonal trend maps. Squares dimension indicates the significance level of the trend: large squares $p < 0.05$, small squares otherwise.

At monthly scale, the majority of the negative trends has been identified, for all the winter months, in the northwestern side of the region, with rainfall reductions lower than −10 mm/10 years largely detected especially in January (Figure 4). On the contrary, positive trends have been evaluated in February in the Ionian side, with a maximum increase higher than 10 mm/10 years (Figure 4).

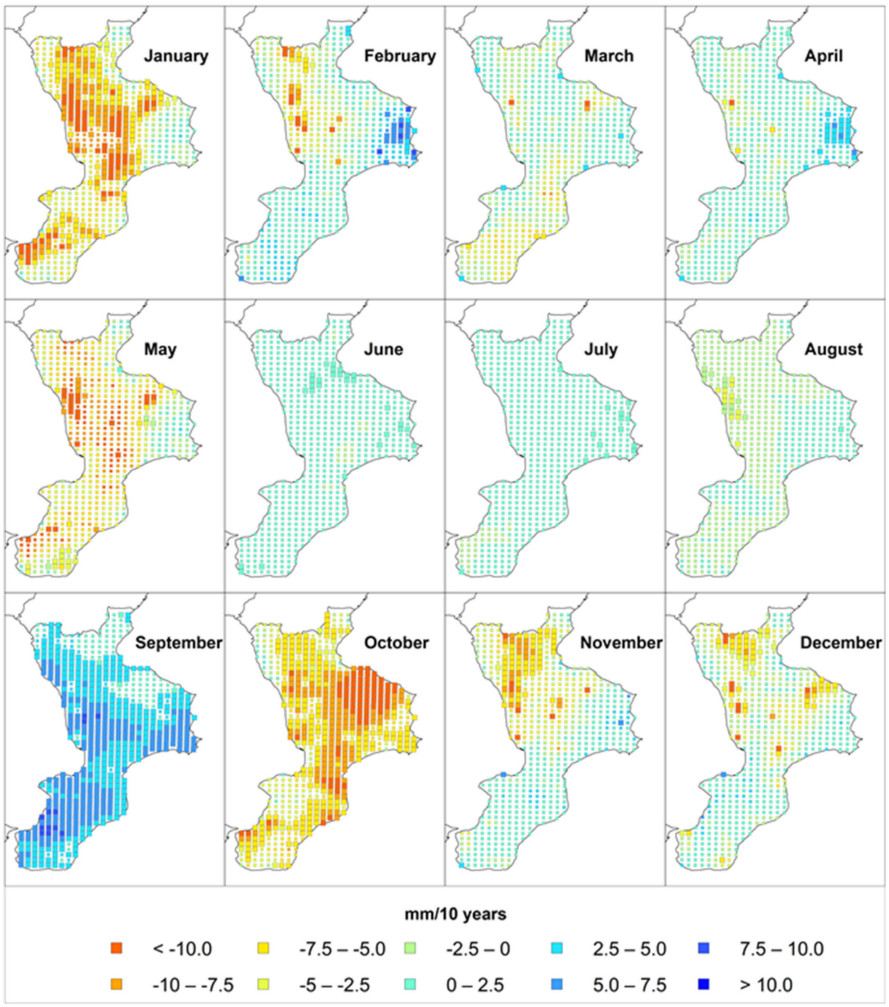

Figure 4. Monthly trend maps. Squares dimension indicates the significance level of the trend: large squares $p < 0.05$, small squares otherwise.

In spring, only about 10% of the grid points showed significant trends with similar percentages between positive and negative values. In fact, 4.8% of the grid points showed a positive trend and 5.8% a negative one (Figure 2a). At a monthly scale, in March, 1.0% of the grid points presented either positive or negative trends (Figure 2a). In April, the majority of the grid series evidenced (Figure 2a) a positive trend (4.6% of the grid points against 0.8% of negative values). Conversely, in May, 8.1% of the grid point showed negative trends and only 0.2% positive ones (Figure 2a). Spatially, in spring, clear opposite trends (but often not significant) have been detected between the two sides of the region: a prevalent negative trend in the western side, reaching also values lower than −20 mm/10 years, and a positive trend in the eastern side, even though with increasing values between 12 and 16 mm/10 years (Figure 3). This trend behavior can also be identified at monthly scale, with positive values (also between 5 and 7.5 mm/10 years) detected in April on the Ionian side of the region and negative trends detected in May, on the Tyrrhenian side, with a maximum reduction lower than −10 mm/10 years (Figure 4).

Differently from winter, summer showed a positive trend even though significant only for 6.3% of the grid points, while negative values have been identified in 0.3% of them (Figure 2a). Additionally at monthly scale, only few grid points evidenced significant trends. In fact, in June and in July a positive tendency has been detected in 4.6% and 2.3% of the series, respectively, while in August both negative (4.0% of the grid points) and positive (0.2%) trends have been identified (Figure 2a).

The spatial results of the trend analysis applied to the summer rainfall allowed to identify positive trends in the eastern side of the region (highest magnitude between 4 and 8 mm/10 years), while the western side showed a significant negative tendency only for two cells with a maximum reduction between −8 and −4 mm/10 years (Figure 3). The positive trends detected in the eastern side of the region have been also identified at monthly scale in June and July, reaching magnitudes not higher than 2.5 mm/10 years, while in August several grid points in the Tyrrhenian side of the region showed negative trend values also between −5 and −2.5 mm/10 years (Figure 4).

Finally, a marked negative trend has been detected in autumn, with 19.7% of the grid points showing a negative trend and only 1 grid point (0.2% of the total) evidencing a positive one (Figure 2a). A sharp contrast emerged in the autumn months. In fact, in September a marked positive trend has been detected in 81.4% of the grid points, while an opposite behavior has been identified in October (67.2% of the cells). In November, both negative (13.3% of the grid points) and positive (0.5%) trends have been detected (Figure 2a). The spatial distribution of the autumn trend is similar to the winter one, even though with less grid points showing a significant trend, but with magnitude reaching −20 mm/10 years. Given the very different percentages of grid points presenting positive or negative trends in September and autumn (Figure 2a), the spatial distribution of the trends in these months is quite the opposite. In fact, in September, positive trend values have been identified across the region and, especially, on the western side with magnitudes higher than 10 mm/10 years. Conversely, in October, the region is affected by negative trends especially in the Ionian side with reductions lower than −10 mm/10 years. Finally, in November, negative trend values lower than −10 mm/10 years have been identified in the northern side of the region (Figure 4).

5. Discussion

Although in literature several gridded databases have been proposed, in this work a gridded database has been built starting from 129 rain gauges distributed on the Calabria region. Due to the high spatial density of the station network, the gridded database has a high spatial resolution (5 km × 5 km) which allows a better spatial analysis of the trend results and allows overcoming some problems that affect the more diffuse global gridded datasets. As an example, Isotta et al. [33] evidenced strengths (e.g., spatial variations, correction of unrealistic spatial features) and weaknesses (e.g., overestimate mean precipitation and wet day frequency) of gridded datasets obtained through regional reanalysis. In particular, as pointed out by Prein and Gobiet [34] the low station density can be considered as one of the major error sources introducing high uncertainty in the gridded products. For example, Rudolf et al. [35] studied the influence of the station density on a 2.5° × 2.5° gridded dataset evaluated over different land regions with high station coverage, evidencing an error between ±7 and 40% when 5 rain gauges per grid cell are considered. Stefanidis et al. [36] compared data of rain gauge stations of the mountainous range of Central Pindus (Greece) with the RCMs simulations in 1974–2000, demonstrating that RCMs gridded data often fail to characterize the temporal variability of rainfall series.

Besides the station density, inhomogeneity has been identified as another important factor affecting the analysis of climate change performed with gridded dataset [37]. Nonetheless, although the interpolation of irregularly spatial distributed station data onto regular grids could be an error source, it is very important and it could present several advantages [34]. For instance, since climate models represent spatial area averages rather than point data, they can be evaluated more directly by using gridded data. Moreover, averaging over regions is straightforward and data become available for ungauged locations.

The results of this study, which evidenced a rainfall reduction in the winter season and a slight increase during summer, confirmed the ones obtained in other southern Italian regions [38–40], while different results have been obtained in other regions of central [41,42] and northern Italy [42]. In fact, in southern Italy the rainfall pattern is similar to that of eastern North Africa, unlike the rest of Italy and much of western Europe which are subject

to the same pattern as the western North Africa [43]. Both local and global factors can be responsible for the trend behavior detected in this study. In fact, locally, the orography of the region seems to impact on the rainfall trends because a different behavior emerged in some seasons between the Ionian and the Tyrrhenian side of the region. In fact, the particular orography of the region, trending south–north, constitutes an important barrier to the mean airflow approaching from the west [44]. Moreover, at global scale, several authors [45,46] evidenced that the trend behaviors in the Euro–Mediterranean area, and thus in the Calabria region, could be connected with to the so-called teleconnection patterns, largely described in literature [47–49]. In particular, several studies [50–52] showed the impacts of the North Atlantic Oscillation (NAO) especially in the western Mediterranean area within which the Calabria region falls. Finally, results of this study slightly disagree with the ones obtained in Brunetti et al. [8] in which more marked trends have been detected. This difference may be due to the changed methodology applied to grid the monthly data and to the different observation period. In fact, in Brunetti et al. [8] the last year of observation is 2006 which is close to the period 2001–2002 in which the Calabria region has been hit by a severe and prolonged drought [53].

6. Conclusions

Results of this study, even though confirming tendencies already evidenced in past analyses referred to the same region and other areas of the Mediterranean basin, have been obtained by means of a gridded data base, with high spatial resolution (5 km $\times$ 5 km). This allowed us to spatially distinguish the various tendencies in a more detailed way than in the past. For this reason, the results could be useful to manage and plan the various sectors strictly influenced by the rainfall distribution and tendencies, i.e., agriculture, water resources, geo-hydrological risk, etc. In particular, the main results concerning the decreasing trends of the annual and winter–autumn rainfall and the increasing trend for the summer one, especially observed in specific territories of the region, could provide important inputs to water management stakeholders, in planning the realization of artificial water reservoirs and the distribution of pipelines. As a future development of this study, a similar gridded data set could be built by means of sub-daily rainfall data with the aim to investigate tendencies of heavy and short rainfall events that can cause damaging hydrogeological events and erosion phenomena.

Author Contributions: Conceptualization, G.P. and R.C.; methodology, G.P.; software, G.P. and T.C.; formal analysis, G.P. and T.C.; validation, T.C. and R.C.; investigation, G.P.; data curation, R.C. and T.C.; writing—original draft preparation, T.C.; writing—review and editing, R.C. and T.C.; visualization, G.P. and T.C.; supervision, R.C. All authors have read and agreed to the published version of the manuscript.

Funding: This study was funded by FORMAS (SE), DLR (DE), BMWFW (AT), IFD (DK), MINECO (ES), ANR (FR) with co-funding by the European Union, Grant number 690462 (INDECIS EU PROJECT).

Institutional Review Board Statement: Not applicable.

Informed Consent Statement: Not applicable.

Data Availability Statement: The data presented in this study are available on request from the corresponding authors.

Conflicts of Interest: The authors declare no conflict of interest.

References

1. IPCC (Intergovernmental Panel on Climate Change). *Climate Change and Land: An IPCC Special Report on Climate Change, Desertification, Land Degradation, Sustainable Land Management, Food Security, and Greenhouse Gas Fluxes in Terrestrial Ecosystems*; IPCC: Geneva, Switzerland, 2019.
2. Giorgi, F. Climate change hot-spots. *Geophys. Res. Lett.* **2006**, *33*, L08707. [CrossRef]
3. Caloiero, T.; Veltri, S.; Caloiero, P.; Frustaci, F. Drought Analysis in Europe and in the Mediterranean Basin Using the Standardized Precipitation Index. *Water* **2018**, *10*, 1043. [CrossRef]

4. Chaouche, K.; Neppel, L.; Dieulin, C.; Pujol, N.; Ladouche, B.; Martin, E.; Salas, D.; Caballero, Y. Analyses of precipitation, temperature and evapotranspiration in a French Mediterranean region in the context of climate change. *Comptes Rendus Geosci.* **2010**, *342*, 234–243. [CrossRef]
5. Valdes-Abellan, J.; Pardo, M.A.; Tenza-Abril, A.J. Observed precipitation trend changes in the western Mediterranean region. *Int. J. Climatol.* **2017**, *37*, 1285–1296. [CrossRef]
6. Caloiero, T.; Coscarelli, R.; Gaudio, R.; Leonardo, G.P. Precipitation trend and concentration in the Sardinia region. *Theor. Appl. Climatol.* **2019**, *137*, 297–307. [CrossRef]
7. Gudmundsson, L.; Seneviratne, S.I. Anthropogenic climate change affects meteorological drought risk in Europe. *Environ. Res. Lett.* **2016**, *11*, 044005. [CrossRef]
8. Brunetti, M.; Caloiero, T.; Coscarelli, R.; Gullà, G.; Nanni, T.; Simolo, C. Precipitation variability and change in the Calabria region (Italy) from a high resolution daily dataset. *Int. J. Clim.* **2012**, *32*, 57–73. [CrossRef]
9. Deitch, M.J.; Sapundjieff, M.J.; Feirer, S.T. Characterizing Precipitation Variability and Trends in the World's Mediterranean-Climate Areas. *Water* **2017**, *9*, 259. [CrossRef]
10. Peña-Angulo, D.; Vicente-Serrano, S.M.; Domínguez-Castro, F.; Murphy, C.; Reig, F.; Tramblay, Y.; Trigo, R.M.; Luna, M.Y.; Turco, M.; Noguera, I.; et al. Long-term precipitation in Southwestern Europe reveals no clear trend attributable to anthropogenic forcing. *Environ. Res. Lett.* **2020**, *15*, 094070. [CrossRef]
11. Llasat, M.C.; Llasat-Botija, M.; Prat, M.; Porcu, F.; Price, C.; Mugnai, A.; Lagouvardos, K.; Kotroni, V.; Katsanos, D.; Michaelides, S.; et al. High-impact floods and flash floods in Mediterranean countries: The flash preliminary database. *Adv. Geosci.* **2010**, *23*, 47–55. [CrossRef]
12. Yao, Y.; Liu, J.; Wang, Z.; Wei, X.; Zhua, H.; Fud, W.; Shao, M. Responses of soil aggregate stability, erodibility and nutrient enrichment to simulated extreme heavy rainfall. *Sci. Total Environ.* **2020**, *709*, 136150. [CrossRef] [PubMed]
13. Polade, S.D.; Gershunov, A.; Cayan, D.R.; Dettinger, M.D.; Pierce, D.W. Precipitation in a warming world: Assessing projected hydro-climate changes in California and other Mediterranean climate regions. *Sci. Rep.* **2017**, *7*, 10783. [CrossRef]
14. Stefanidis, S.; Stathis, D. Spatial and Temporal Rainfall Variability over the Mountainous Central Pindus (Greece). *Climate* **2018**, *6*, 75. [CrossRef]
15. Gulizia, C.; Camilloni, I.A. Spatio-temporal comparative study of the representation of pre-cipitation over South America derived by three gridded datasets. *Int. J. Climatol.* **2015**, *36*, 1549–1559. [CrossRef]
16. Faiz, M.A.; Liu, D.; Fu, Q.; Sun, Q.; Li, M.; Baig, F.; Li, T.; Cui, S. How accurate are the performances of gridded precipitation data products over Northeast China? *Atmos. Res.* **2018**, *211*, 12–20. [CrossRef]
17. Singh, H.; Najafi, M.R. Evaluation of gridded climate datasets over Canada using univariate and bivariate approaches: Implications for hydrological modelling. *J. Hydrol.* **2020**, *584*, 124673. [CrossRef]
18. Sidău, M.R.; Croitoru, A.-E.; Alexandru, D.-E. Comparative Analysis between Daily Extreme Temperature and Precipitation Values Derived from Observations and Gridded Datasets in North-Western Romania. *Atmosphere* **2021**, *12*, 361. [CrossRef]
19. Darand, M.; Khandu, K. Statistical Evaluation of Gridded Precipitation Datasets Using Rain Gauge Observations over Iran. *J. Arid Environ.* **2020**, *178*, 104172. [CrossRef]
20. Yao, J.; Chen, Y.; Yu, X.; Zhao, Y.; Guan, X.; Yang, L. Evaluation of multiple gridded precipitation datasets for the arid region of northwestern China. *Atmos. Res.* **2020**, *236*, 104818. [CrossRef]
21. Abdourahamane, Z.S. Evaluation of fine resolution gridded rainfall datasets over a dense network of rain gauges in Niger. *Atmos. Res.* **2021**, *252*, 105459. [CrossRef]
22. Aouissi, J.; Benabdallah, S.; Lili Chabaâne, Z.; Cudennec, C. Valuing Scarce Observation of Rainfall Variability with Flexible Semi-Distributed Hydrological Modelling—Mountainous Mediterranean Context. *Sci. Total Environ.* **2018**, *643*, 346–356. [CrossRef]
23. Caroletti, G.N.; Coscarelli, R.; Caloiero, T. Validation of Satellite, Reanalysis and RCM Data of Monthly Rainfall in Calabria (Southern Italy). *Remote Sens.* **2019**, *11*, 1625. [CrossRef]
24. Köppen, W. *Das Geographische System der Klimate. Handbuch der Klimatologie*; Köppen, W., Geiger, R., Eds.; Verlag von Gebrüder Borntraeger: Berlin, Germany, 1936; Volume 1, Part C; pp. 1–44.
25. Caloiero, T.; Pasqua, A.A.; Petrucci, O. Damaging Hydrogeological Events: A Procedure for the Assessment of Severity Levels and an Application to Calabria (Southern Italy). *Water* **2014**, *6*, 3652–3670. [CrossRef]
26. Shepard, D.S. A two-dimensional interpolation function for irregularly-spaced data. In Proceedings of the 1968 ACM National Conference, Las Vegas, NV, USA, 27–29 August 1968.
27. Shepard, D.S. Computer Mapping: The SYMAP Interpolation Algorithm. In *Spatial Statistics and Models*; Gaile, G.L., Willmott, C.J., Eds.; Springer: New York, NY, USA, 1984; pp. 133–145.
28. Dirks, K.N.; Hay, J.E.; Stow, C.D.; Harris, D. High-resolution studies of rainfall on Norfolk Island. Part 2: Interpolation of rainfall data. *J. Hydrol.* **1998**, *208*, 187–193. [CrossRef]
29. Pellicone, G.; Caloiero, T.; Modica, G.; Guagliardi, I. Application of several spatial interpolation techniques to monthly rainfall data in the Calabria region (southern Italy). *Int. J. Climatol.* **2018**, *38*, 3651–3666. [CrossRef]
30. Sen, P.K. Estimates of the regression coefficient based on Kendall's tau. *J. Am. Stat. Assoc.* **1968**, *63*, 1379–1389. [CrossRef]
31. Mann, H.B. Nonparametric tests against trend. *Econometrica* **1945**, *13*, 245–259. [CrossRef]
32. Kendall, M.G. *Rank Correlation Methods*; Hafner Publishing Company: New York, NY, USA, 1962.

33. Isotta, F.A.; Vogel, R.; Frei, C. Evaluation of European regional reanalyses and downscalings for precipitation in the Alpine region. *Meteorol. Z.* **2015**, *24*, 15–37. [CrossRef]
34. Prein, A.F.; Gobiet, A. Impacts of uncertainties in European gridded precipitation observations on regional climate analysis. *Int. J. Climatol.* **2017**, *37*, 305–327. [CrossRef] [PubMed]
35. Rudolf, B.; Hauschild, H.; Rueth, W.; Schneider, U. Terrestrial precipitation analysis: Operational method and required density of point measurements. In *Global Precipitation and Climate Change*; Desbois, M., Desalmand, F., Eds.; Springer: Berlin/Heidelberg, Germany, 1994; pp. 173–186.
36. Stefanidis, S.; Dafis, S.; Stathis, D. Evaluation of Regional Climate Models (RCMs) Performance in Simulating Seasonal Precipitation over Mountainous Central Pindus (Greece). *Water* **2020**, *12*, 2750. [CrossRef]
37. New, M.; Hulme, M.; Jones, P. Representing Twentieth-Century Space–Time Climate Variability. Part I: Development of a 1961–90 Mean Monthly Terrestrial Climatology. *J. Clim.* **1999**, *12*, 829–856. [CrossRef]
38. Longobardi, A.; Villani, P. Trend Analysis of Annual and Seasonal Rainfall Time Series in the Mediterranean Area. *Int. J. Climatol.* **2010**, *30*, 1538–1546. [CrossRef]
39. Diodato, N. Climatic fluctuations in southern Italy since 17th century: Reconstruction with precipitation records at Benevento. *Clim. Change* **2007**, *80*, 411–431. [CrossRef]
40. Caloiero, T.; Coscarelli, R.; Ferrari, E. Assessment of seasonal and annual rainfall trend in Calabria (southern Italy) with the ITA method. *J. Hydroinform.* **2020**, *22*, 738–748. [CrossRef]
41. Bartolini, G.; Grifoni, D.; Magno, R.; Torrigiani, T.; Gozzini, B. Changes in temporal distribution of precipitation in a Mediterranean area (Tuscany, Italy) 1955–2013. *Int. J. Clim.* **2018**, *38*, 1366–1374. [CrossRef]
42. Pavan, V.; Antolini, G.; Barbiero, R.; Berni, N.; Brunier, F.; Cacciamani, C.; Cagnati, A.; Cazzuli, O.; Cicogna, A.; De Luigi, C.; et al. High resolution climate precipitation analysis for north-central Italy, 1961–2015. *Clim. Dyn.* **2019**, *52*, 3435–3453. [CrossRef]
43. Pinault, J.L. Global warming and rainfall oscillation in the 5–10 yr band in Western Europe and Eastern North America. *Clim. Change* **2012**, *114*, 621–650. [CrossRef]
44. Caloiero, T.; Callegari, G.; Cantasano, N.; Coletta, V.; Pellicone, G.; Veltri, A. Bioclimatic analysis in a region of southern Italy (Calabria). *Plant Biosyst.* **2015**, *150*, 1282–1295. [CrossRef]
45. Fleig, A.K.; Tallaksen, L.M.; James, P.; Hisdal, H.; Stahl, K. Attribution of European precipitation and temperature trends to changes in synoptic circulation. *Hydrol. Earth Syst. Sci.* **2015**, *19*, 3093–3107. [CrossRef]
46. Hoy, A.; Schucknecht, A.; Sepp, M.; Matschullat, J. Large-scale synoptic types and their impact on European precipitation. *Theor. Appl. Climatol.* **2014**, *116*, 19–35. [CrossRef]
47. Wallace, J.M.; Gutzler, D.S. Teleconnections in the Geopotential Height Field during the Northern Hemisphere Winter. *Mon. Weather Rev.* **1981**, *109*, 784–812. [CrossRef]
48. Barnston, A.G.; Livezey, R.E. Classification, seasonality and persistence of low-frequency atmospheric circulation patterns. *Mon. Weather Rev.* **1987**, *115*, 1083–1126. [CrossRef]
49. Rogers, J.C. Patterns of low-frequency monthly sea-level pressure variability (1899–1986) and associated wave cyclone frequencies. *J. Clim.* **1990**, *3*, 1364–1379. [CrossRef]
50. Trigo, I.F.; Davies, T.D.; Bigg, G.R. Decline in Mediterranean rainfall caused by weakening of mediterranean cyclones. *Geophys. Res. Lett.* **2000**, *27*, 2913–2916. [CrossRef]
51. Caloiero, T.; Coscarelli, R.; Ferrari, E.; Mancini, M. Precipitation change in Southern Italy linked to global scale oscillation indexes. *Nat. Hazards Earth Syst. Sci.* **2011**, *11*, 1–12. [CrossRef]
52. Ferrari, E.; Caloiero, T.; Coscarelli, R. Influence of the North Atlantic Oscillation on winter rainfall in Calabria (southern Italy). *Theor. Appl. Climatol.* **2013**, *114*, 479–494. [CrossRef]
53. Buttafuoco, G.; Caloiero, T. Drought events at different timescales in southern Italy (Calabria). *J. Maps* **2014**, *10*, 529–537. [CrossRef]